



Cite this: *Phys. Chem. Chem. Phys.*,
2019, 21, 12611

High bond difference parameter-induced low thermal transmission in carbon allotropes with sp^2 and sp^3 hybridization†

Zhihao Feng,^{ab} Huicong Dong,^{ID *ab} Shenghong Ju,^c Bin Wen,^{*b} Yuwen Zhang^d and Roderick Melnik^e

Carbon allotropes play an important role in the thermal transmission field, while there are huge thermal differences in their thermal conductivities. In this work, thermal transmission in three novel carbon allotropes with sp^2 and sp^3 hybridization has been studied, including T6-carbon, T10 and 3D-C5 by using non-equilibrium molecular dynamic simulations and phonon kinetic theory. Graphene and diamond with standard sp^2 and sp^3 hybridization, respectively, are also examined for comparison. Our results indicate that the thermal conductivities of T6-carbon, T10 and 3D-C5 at room temperature are much lower than those of diamond and graphene. Phonon kinetic theory analysis shows that the lower thermal conductivity of T6-carbon, T10 and 3D-C5 is caused by the combined action of their reduced phonon group velocities and relaxation time. Moreover, the bond difference parameter has been proposed to describe the relationship between bond structures and thermal conductivity in carbon allotropes, which presents a new and convenient method for in-depth understanding the thermal conductivity of carbon allotropes.

Received 21st February 2019,
Accepted 11th May 2019

DOI: 10.1039/c9cp01029g

rsc.li/pccp

1. Introduction

As one of the most significant and fundamental properties of materials, thermal conductivity is applied to characterize phonon scattering properties in materials for many technological applications.^{1–3} Due to diverse structures,^{4–6} thermal conductivity of materials varies greatly, thus, leading to quite different application fields. Materials with high thermal conductivity are usually used in cooling microelectronics for passive heat spreading,⁷ while those with low thermal conductivity are commonly used in thermoelectric devices to increase thermal conversion.^{8,9}

As for thermal transport properties, carbon allotropes, with flexibility of bond hybridizations, have attracted a great deal of special interest, since their thermal conductivity can span an extraordinary large range of five orders of magnitude.¹⁰ It is

well known that diamond and graphene, the two most famous carbon allotropes, both exhibit high thermal transmission.^{11–15} However despite both of them having high thermal conductivity, their bond hybridizations are rather different, which is totally standard sp^3 hybridization for diamond, while totally standard sp^2 hybridization for graphene. However, whether the carbon allotropes with mixed sp^2 and sp^3 hybridization can also possess high thermal conductivity, and how the phonon properties and bond properties will affect their thermal transmission still need to be investigated, which will also be meaningful for the design of new carbon allotropes with diverse thermal properties.

To clear this issue, in this paper, the thermal transport properties of carbon allotropes with different ratios of mixed sp^2 and sp^3 hybridization, including T6-carbon,¹⁶ T10¹⁷ and 3D-C5,¹⁸ were studied by applying non-equilibrium molecular dynamics (NEMD) simulation and phonon kinetic theory. For comparison, thermal transmission in diamond and graphene was also studied. The simulated results indicate that carbon allotropes with mixed sp^2 and sp^3 hybridization, including T6, T10 and 3D-C5, show a much lower thermal conductivity when compared with diamond and graphene, which is due to high bond difference parameters.

2. Theory and methodology

The atomic configurations of T6-carbon, T10 and 3D-C5, as well as that of diamond and graphene are depicted in Fig. 1, and

^a Hebei Key Laboratory of Material Near-net Forming Technology, Hebei University of Science and Technology, Shijiazhuang, Hebei, 050000, China.

E-mail: donghuicong00@163.com

^b State Key Laboratory of Metastable Materials Science and Technology, Yanshan University, Qinhuangdao 066004, China. E-mail: wenbin@ysu.edu.cn

^c Department of Mechanical Engineering, The University of Tokyo, 7-3-1 Hongo, Bunkyo, Tokyo 113-8656, Japan

^d Department of Mechanical and Aerospace Engineering, University of Missouri-Columbia, Columbia, Missouri, USA

^e The MS2 Discovery Interdisciplinary Research Institute, Wilfrid Laurier University, 75 University Ave. West, Waterloo, Ontario N2L 3C5, Canada

† Electronic supplementary information (ESI) available. See DOI: 10.1039/c9cp01029g

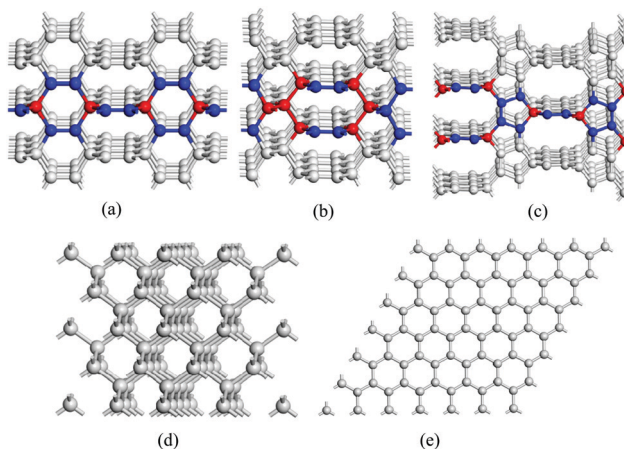


Fig. 1 Atomic configuration of (a) T6-carbon, (b) T10, (c) 3D-C5, (d) diamond and (e) graphene, respectively. In (a–c), the red atoms represent carbon atoms with sp^3 hybridization and the blue atoms represent atoms with sp^2 hybridization.

their structural details are listed in Table 1. All of the three new carbon allotropes, including T6-carbon, T10 and 3D-C5, are composed of sp^2 and sp^3 hybridization, and some representatives for sp^2 -hybridized (the red) atoms and sp^3 -hybridized (the blue) atoms are shown in Fig. 1(a–c). To avoid the effect of size perpendicular to the heat flux direction, in simulation, the model length varies from 30 nm to 120 nm in x , y , and z directions for these five structures, and the cross section has been set at about 3 nm \times 3 nm.

In this work, NEMD simulations^{19,20} are performed to calculate the thermal conductivity of T6-carbon, T10, 3D-C5, diamond and graphene by using Large-scale Atomic/Molecular Massively Parallel (LAMMPS),²¹ which is performed by following Fourier's law (details can be seen in the ESI,† Discussion 1)

$$J = -KdT/dx, \quad (1)$$

where K is the thermal conductivity, dT/dx is the temperature gradient averaged over time and space, and J is the heat current. In simulation, the Tersoff potential^{22,23} is employed to describe interactions of carbon–carbon atoms, which has been successfully used in many carbon-based systems, such as diamond,¹¹ graphene²⁴ and carbon nanotubes²⁵ for studying thermal and mechanical properties. The integration time step is set at 0.5 fs, and a periodic boundary condition has been

Table 1 The space group, lattice constant (Å), density ($g\text{ cm}^{-3}$) and ratio of sp^3 atoms of T6-carbon, T10, 3D-C5, diamond and graphene

Name	Space group	Lattice constant (Å)	Mass density ($g\text{ cm}^{-3}$)	Ratio (%)
T6-carbon ¹⁶	$P4_2/mmc$	$a = 2.6$ $c = 6$	2.95	33
T10 ¹⁷	$P4_2/mmc$	$a = 2.5577$ $c = 9.6009$	3.157	60
3D-C5 ¹⁸	$I4_1/amd$	$a = 3.7111$ $c = 13.2956$	2.178	20
Diamond ¹⁷	$Fd\bar{3}m$	$a = 3.54$	3.55	100
Graphene ¹³	$P6_3/mmc$	$a = 2.46$	2.24	0

applied to all three directions to eliminate the size effect. The atomic structures of these five phases are firstly equilibrated at room temperature for 400 ps using the isothermal isobaric ensemble (*NPT*) at atmospheric pressure. After this, a heat flux is imposed on the relaxed systems. To obtain a steady state, we have run 10^6 time steps. At each time step, a small amount of heat is added into a thin slab of thickness 2δ in the middle region (hot region) and removed from the thin slabs of thickness δ at the two ends (the cold region) as shown in Fig. S1(a) (ESI,†), so as to ensure the heat addition and removal by exchanging the velocity of the lowest kinetic energy atoms in the hot region with that of the highest kinetic energy atoms in the cold region. To obtain the temperature gradient, the simulated model is divided into 100 slabs with a thickness of δ , and the time interval of velocity exchange has been set at 50 ps. After reaching a steady state, the temperature gradient can be obtained, which can be seen in Fig. S1(b) (ESI,†). As noted in a previous study, because of the finite size effect, the temperature profile is nonlinear near the hot and cold ends.^{26–29} Under these conditions, to avoid edge effects and obtain correct thermal conductivity, the middle part of the temperature gradient, which is labeled red in the temperature profile, was taken to calculate thermal conductivity by using eqn (1).³⁰

3. Results and discussion

3.1 Thermodynamic stability of carbon allotropes

To identify the thermodynamic stability of these carbon allotropes, PHONOPY has been implemented³¹ in combination with the VASP to calculate the phonon dispersion and phonon density of states (refer to the ESI,† Discussion 2), which is in agreement with the neutron inelastic scattering and Raman data,³² and the calculated results can also well coincide with the results using the Tersoff potential as shown in Fig. S2 (ESI,†). In Fig. 2, it can be seen that there is no imaginary frequency in the entire phonon dispersions for all allotropes, confirming the kinetic stability of these structures. From Fig. 2(a–c), we can see that the highest phonon frequency of T6-carbon, T10 and 3D-C5 can reach about 50 THz, even slightly higher than that of diamond in Fig. 2(d) and graphene in Fig. 2(e). It is worth noting that there exists a large phonon gap of about 9 THz in T6-carbon, a phonon gap of 5 THz in T10, and a little gap of 2 THz in 3D-C5 between high frequency optical phonons and middle and low frequency optical phonons. However for diamond and graphene, there are no phonon gaps in their phonon spectra. All of the above simulated results here are consistent with previous studies.^{16–18,33}

3.2 Thermal conductivity from NEMD simulations

To validate our approach, the thermal conductivity of diamond and graphene was calculated, firstly. Based on the kinetic theory of phonon transport, the reverse of thermal conductivity is linearly proportional to the reverse of the sample length,³⁴ which is given by

$$\frac{1}{K} = \frac{1}{K_\infty} \left(\frac{l_{SL}}{L} + 1 \right) \quad (2)$$

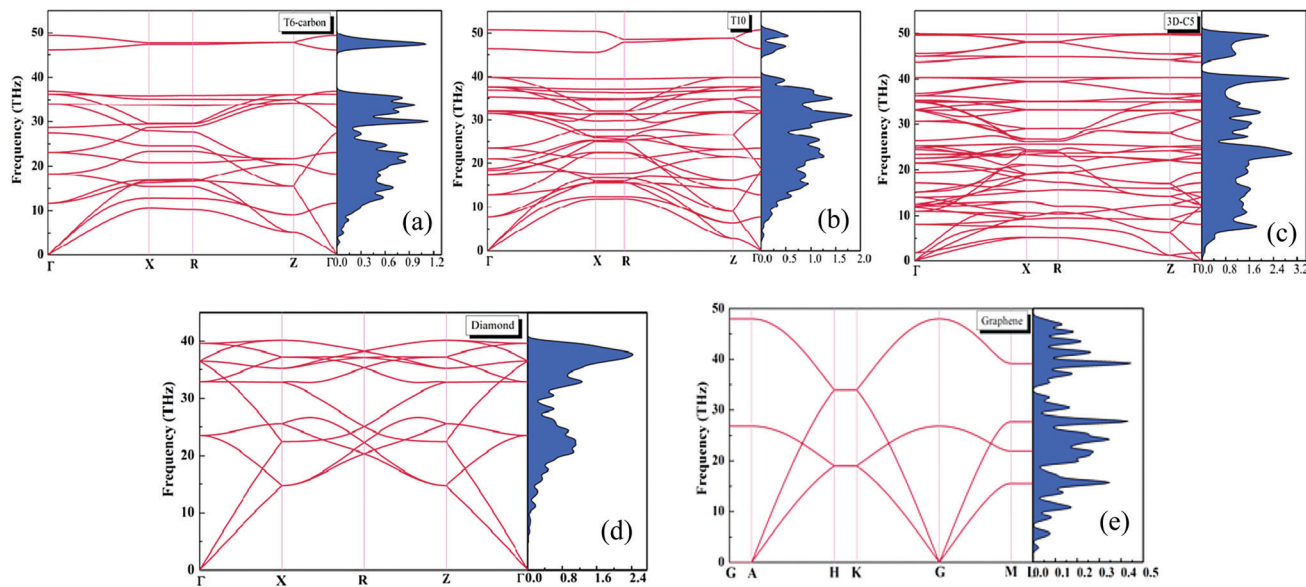


Fig. 2 Phonon dispersion and phonon density of states (DOS) of (a) T6-carbon, (b) T10, (c) 3D-C5, (d) diamond and (e) graphene.

where K_∞ is the thermal conductivity of the bulk material, l_{SL} is the effective phonon mean free path in the bulk crystal. Thus, by extrapolating the linear relationship, the thermal conductivity of bulk materials can be calculated, as can be seen in Fig. 3(a). In this method, the thermal conductivity of bulk diamond ($1415 \text{ W m}^{-1} \text{ K}^{-1}$) and graphene ($2272 \text{ W m}^{-1} \text{ K}^{-1}$, where the thickness of graphene is set at 3.45 \AA) can be obtained, as shown in Fig. 3(b), which is consistent with previous results,^{11,13} demonstrating the correctness of parameters selected in thermal conductivity simulation.

By applying the same method and parameters, the thermal conductivities of T6-carbon, T10 and 3D-C5 with different model lengths are calculated along three different directions, [100] [010] and [001]. Fig. 3(a) only shows linear relationships along the [001] direction of the three structures as an illustration. By extrapolating, it can be observed that the thermal conductivities

for T6-carbon, T10 and 3D-C5 along the [001] direction are $234 \text{ W m}^{-1} \text{ K}^{-1}$, $161 \text{ W m}^{-1} \text{ K}^{-1}$ and $67 \text{ W m}^{-1} \text{ K}^{-1}$, respectively. Fig. 3(b) shows the thermal conductivity of the above three structures in different directions. Due to symmetry in the [100] and [010] directions for T6-carbon, T10 and 3D-C5, the same thermal conductivity was obtained in the [100] and [010] directions for all the three structures, and in Fig. 3(b) we only show their thermal conductivities along the [100] and [001] directions, as well as their average thermal conductivities K_{ave} in the inset. As can be seen, the calculated thermal conductivities for T6-carbon along the [100] and [001] directions are $K_{[100]} = 309 \text{ W m}^{-1} \text{ K}^{-1}$, $K_{[001]} = 234 \text{ W m}^{-1} \text{ K}^{-1}$, and the average thermal conductivity $K_{\text{ave}} = 284 \text{ W m}^{-1} \text{ K}^{-1}$. For T10, $K_{[100]} = 505 \text{ W m}^{-1} \text{ K}^{-1}$, $K_{[001]} = 161 \text{ W m}^{-1} \text{ K}^{-1}$, and $K_{\text{ave}} = 390 \text{ W m}^{-1} \text{ K}^{-1}$. For 3D-C5, $K_{[100]} = 17 \text{ W m}^{-1} \text{ K}^{-1}$, $K_{[001]} = 67 \text{ W m}^{-1} \text{ K}^{-1}$, and $K_{\text{ave}} = 34 \text{ W m}^{-1} \text{ K}^{-1}$. Comparison of their thermal conductivities shows that although

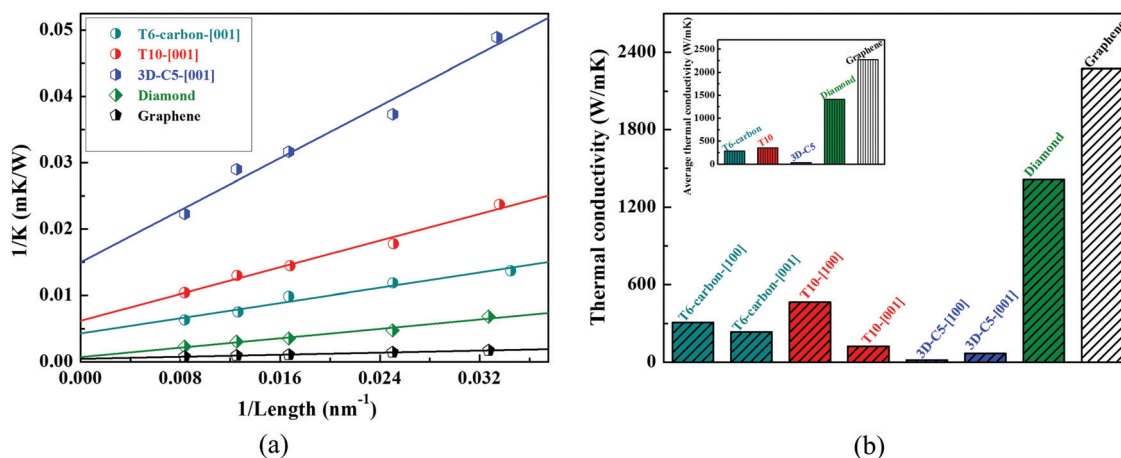


Fig. 3 (a) Length-dependent thermal conductivity of T6-carbon, T10, and 3D-C5 in the [001] direction, as well as that of diamond and graphene at room temperature. (b) Comparison of thermal conductivity for T6-carbon, T10, and 3D-C5 along [100] and [001], as well as that for diamond and graphene at 300 K. Inset: The average thermal conductivity of T6-carbon, T10, 3D-C5, diamond and graphene at 300 K.

they are all composed of sp^2 and sp^3 hybridization, their thermal conductivities are rather different. In particular, the average thermal conductivity of T10 is larger than ten times that of 3D-C5. It is noteworthy that all of their thermal conductivities are much lower than that of diamond with all standard sp^3 hybridization and that of graphene with all standard sp^2 hybridization.

3.3 Phonon kinetic theory analysis for thermal transmission

To explore the lower thermal transmission in T6-carbon, T10 and 3D-C5, phonon kinetic theory,³⁵ depending on the phonon spectra and phonon density of states in Fig. 2, has been used, and it is expressed as:

$$K = \frac{1}{3} C_V v_g l = \frac{1}{3} C_V v_g^2 \tau \quad (3)$$

where K is the thermal conductivity, C_V is the specific capacity, v_g is the phonon group velocity, l is the phonon mean free path, and τ is the relaxation time.

3.3.1 Specific heat capacity analysis. According to phonon kinetic theory, the specific capacity C_V of T6-carbon, T10, and 3D-C5, as well as diamond and graphene has been firstly calculated, as shown in Fig. S3 (ESI†). It can be seen that with the temperature increasing from 0 K to 2000 K, their specific capacities are all increased, and certain values of C_V of T6-carbon, T10, 3D-C5, diamond and graphene at 300 K are listed in Table 2. Comparison shows that their specific capacities are close to each other, even the values for T6-carbon, T10, and 3D-C5 are a little higher than those of diamond and graphene. Thus, the lower thermal conductivity of T6-carbon, T10 and 3D-C5 is essentially unrelated to specific capacity when compared with those of diamond and graphene.

3.3.2 Phonon group velocity analysis. Fig. 4(a–c) show the group velocities for T6-carbon, T10 and 3D-C5 along [100] and [001] directions, respectively, and they are all compared with those of diamond in Fig. 4(d) and graphene in Fig. 4(e). Due to the primary roles of phonon dispersion of acoustic branches in thermal transmission, in this work, we only present one longitudinal and two degenerated transverse modes for the above five carbon allotropes. Here, the phonon group velocity is calculated according to the following relationship:³⁶

$$v_g = (\partial w / \partial q) \quad (4)$$

where q is the wave vector, and w is the frequency of acoustic branches in the phonon spectra. It can be seen that the group velocities vary at different frequencies. In Fig. 4(a), for T6-carbon

Table 2 Calculated specific capacity C_V , average phonon group velocity \bar{v}_g , average phonon group velocity \bar{v}_p , and average values of the square of Grüneisen parameters $\bar{\gamma}^2$ for T6-carbon, T10, 3D-C5, diamond and graphene

	T6-carbon	T10	3D-C5	Diamond	Graphene
C_V (J Km ⁻³)	2.11	2.08	1.68	1.81	1.49
\bar{v}_g (m s ⁻¹)	7076	6829	4007	11 557	9360
\bar{v}_p (m s ⁻¹)	9387	9397	6108	12 300	11 911
$\bar{\gamma}^2$	0.9	1.79	11.78	0.71	0.13

in the [100] direction, the phonon group velocity v_g varies from 231 m s⁻¹ to 11 436 m s⁻¹, and the average group velocity in the [100] direction $\bar{v}_{g[100]}$ is 6532 m s⁻¹. For the [001] direction, v_g varies from 444 m s⁻¹ to 18 960 m s⁻¹, and the average group velocity in the [001] direction $\bar{v}_{g[001]}$ is 8136 m s⁻¹. The average group velocity in three directions for T6-carbon \bar{v}_{g-T6} is 7067 m s⁻¹. Fig. 4(b) and (c) show the phonon group velocities of T10 and 3D-C5 at different frequencies and different directions, and much lower v_g values can also be observed for two of them when compared with those of diamond and graphene. For T10, $\bar{v}_{g[001]}$ is 7604 m s⁻¹, $\bar{v}_{g[100]}$ is 6441 m s⁻¹, and average group velocity \bar{v}_{g-T10} is 6829 m s⁻¹. For 3D-C5, $\bar{v}_{g[001]}$ is 3474 m s⁻¹, $\bar{v}_{g[100]}$ is 4274 m s⁻¹, and its average group velocity $\bar{v}_{g-3D-C5}$ is 4007 m s⁻¹. However for diamond in Fig. 4(d) and graphene in Fig. 4(e), the average group velocity is much higher, which is 11 557 m s⁻¹ for diamond \bar{v}_{g-Dia} and 9360 m s⁻¹ for graphene \bar{v}_{g-Gra} . Notably, the group velocities in T6-carbon, T10 and 3D-C5 also show anisotropy, which is consistent with their anisotropic thermal conductivity.

All the average group velocities \bar{v}_g for the five carbon allotropes are listed in Table 2. Comparison of the average group velocities of T6-carbon, T10, and 3D-C5 with those of diamond and graphene shows that $\bar{v}_{g-T6}^2 / \bar{v}_{g-Dia}^2$ is 0.37, $\bar{v}_{g-T10}^2 / \bar{v}_{g-Dia}^2$ is 0.35, and $\bar{v}_{g-3D-C5}^2 / \bar{v}_{g-Dia}^2$ is only 0.12, while the ratio of the group velocity of T6-carbon, T10, and 3D-C5 and that of graphene is a little higher, $\bar{v}_{g-T6}^2 / \bar{v}_{g-Gra}^2$ is 0.57, $\bar{v}_{g-T10}^2 / \bar{v}_{g-Gra}^2$ is 0.53, and $\bar{v}_{g-3D-C5}^2 / \bar{v}_{g-Gra}^2$ is 0.18. Thus, it can be concluded that the lower group velocities make a great contribution to the lower thermal conductivities of T6-carbon, T10 and 3D-C5 when compared with those of diamond and graphene.

3.3.3 Phonon relaxation time analysis. According to eqn (4), besides volume heat capacity and phonon group velocity, relaxation time is another vital factor that affects thermal transmission in semiconductor materials. By applying semi-empirical theory, the relaxation time τ can be calculated using the following expression:^{37,38}

$$\tau(w) = A \frac{M \bar{v}_g v_p^2}{k_B a y^2 \omega^2 T} \quad (5)$$

In eqn (4), A is a parameter related to the intrinsic material properties, and it varies in different material systems while being invariable in the same material system,^{37,38} M is the average mass of the cell, and the phonon group and phase velocities are denoted as v_g and v_p , respectively; k_B is the Boltzmann constant, a^3 is the volume per atom, ω refers to the phonon frequency at each branch, T denotes temperature, and the mode-Grüneisen parameter is given by γ , which is computed by:³⁹

$$\gamma(\omega) = -\frac{V_0}{\omega_j(q)} \frac{\partial \omega_j(q)}{\partial V_0} \quad (6)$$

where V_0 is the equilibrium volume, j is the phonon branch index, and q is the wave vector. According to eqn (4), in this work, for the five carbon allotropes belonging to the same material system, the values of A , M , k_B and a are all the same, and the difference in their relaxation times is caused by the difference in the group velocity, phase velocity, Grüneisen parameter and

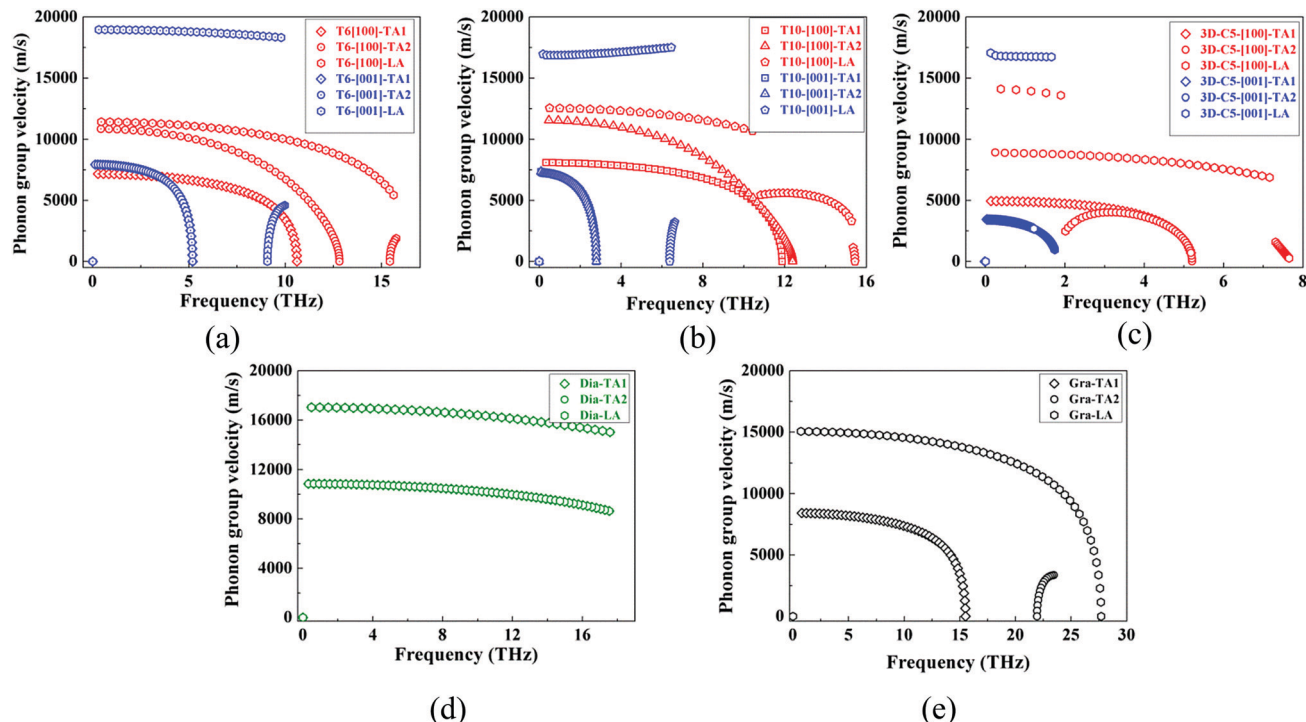


Fig. 4 Phonon group velocities of acoustic branches, including TA1, TA2 and LA for (a) T6-carbon, (b) T10, (c) 3D-C5 along [100] and [001], as well as that for (d) diamond and (e) graphene.

phonon frequency. In addition, in this part, only the acoustic branches in the phonon spectra of the five carbon allotropes are used.

Fig. 5(a–c) show the phonon-dependent phase velocities of one longitudinal and two degenerated transverse branches for T6-carbon, T10, and 3D-C5 along [001] and [100], and those of diamond and graphene are shown in Fig. 5(d) and (e). Comparison shows that the phase velocities of T6-carbon, T10 and 3D-C5 are lower when compared with those of diamond and graphene. By averaging the phase velocities at different frequencies and different directions, the average phase group velocity \bar{v}_p for T6-carbon is 9387 m s^{-1} , for T10 \bar{v}_p is 9397 m s^{-1} , and for 3D-C5 \bar{v}_p is 6108 m s^{-1} , and the average phase velocities of diamond and graphene are much higher, for diamond the value is $12\,300 \text{ m s}^{-1}$, and for graphene is $11\,911 \text{ m s}^{-1}$. The average phase velocities can also be found in Table 2.

To compare the relaxation time of T6-carbon, T10, and 3D-C5 with that of diamond and graphene, the Grüneisen parameters γ were also calculated, and the obtained γ^2 at different frequencies for T6-carbon, T10, 3D-C5, diamond and graphene are plotted in Fig. 6(a)–(e), respectively. It can be seen that when compared with diamond and graphene, the Grüneisen parameters of T6-carbon, T10 and 3D-C5 are much higher. In particular, the values of γ^2 for graphene at different frequencies are all lower than 0.2. By averaging all the γ^2 values at different frequencies and different directions, the average values of the square of Grüneisen parameters $\bar{\gamma}^2$ can be calculated, and the results are listed in Table 2.

By applying the calculated average values of group velocity \bar{v}_g , phase velocity \bar{v}_p , and the square of Grüneisen parameters

$\bar{\gamma}^2$ in Table 2, as well as the average value of phonon frequencies in acoustic branches, the difference between the relaxation times of T6-carbon (τ_{T6}), T10 (τ_{T10}), and 3D-C5 (τ_{3D-C5}) and those of diamond (τ_{Dia}) and graphene (τ_{Gra}) can be obtained. The ratios of the relaxation times of T6-carbon, T10, and 3D-C5 to that of diamond are respectively $\tau_{T6}/\tau_{Dia} = 0.44$, $\tau_{T10}/\tau_{Dia} = 0.25$, and $\tau_{3D-C5}/\tau_{Dia} = 0.04$. The ratios of the relaxation times of T6-carbon, T10, and 3D-C5 to that of graphene are respectively $\tau_{T6}/\tau_{Gra} = 0.26$, $\tau_{T10}/\tau_{Gra} = 0.14$, and $\tau_{3D-C5}/\tau_{Gra} = 0.026$. By both considering the effects of group velocities and relaxation times, it can be deduced that when compared with diamond and graphene, the lower thermal conductivities of T6-carbon, T10 and 3D-C5 are caused by the combined action of reduced group velocities and relaxation times. For T6-carbon, the comparison with diamond indicates that the reduced group velocity plays a more dominant role in its reduced thermal conductivity, while when compared with graphene, the reduced relaxation time is more important. However for T10 and 3D-C5, their reduced relaxation times are dominant to their lower thermal conductivity when compared with those of diamond and graphene.

3.4 Bond difference parameters

It is well known that the properties of materials are fundamentally determined by their structures, namely the element types and chemical bonds. In our work, carbon allotropes including T6-carbon, T10, 3D-C5, diamond and graphene are all made up of the element carbon; thus, the rather different thermal conductivities are caused by the different properties of chemical bonds. Here, the effects of bond length and bond

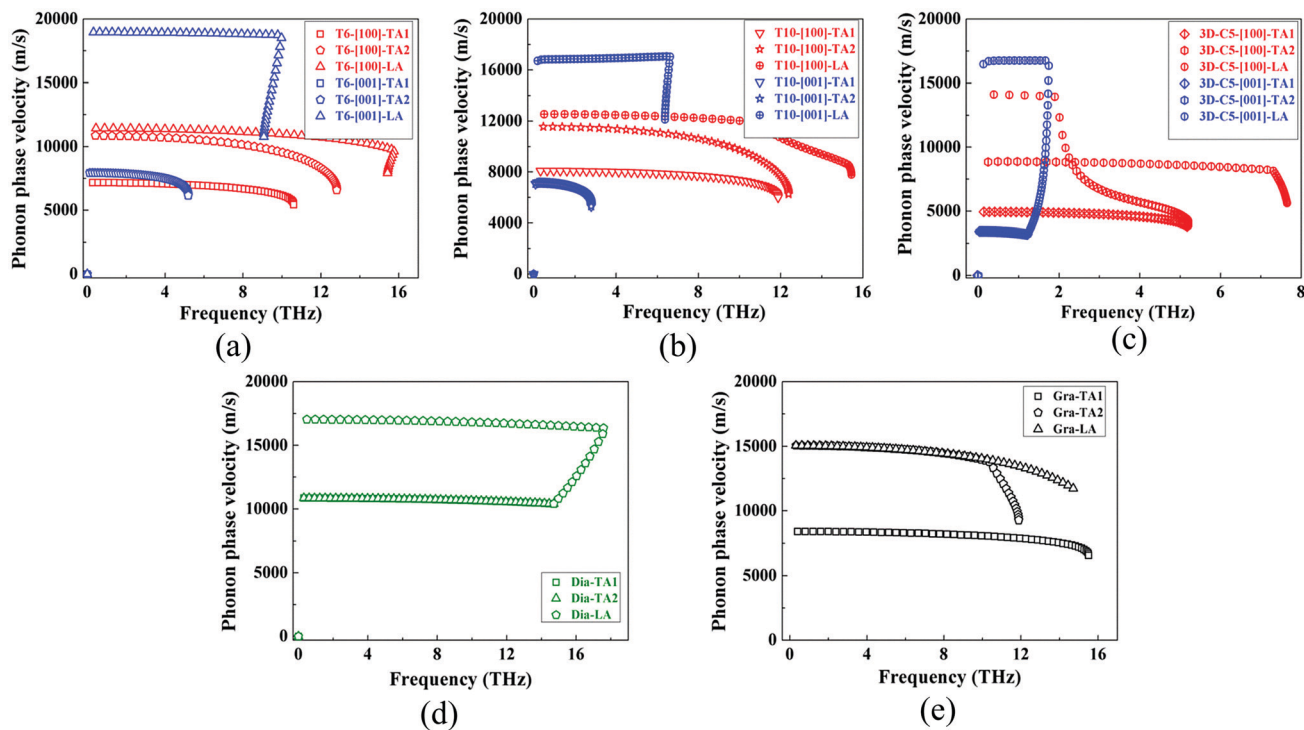


Fig. 5 Phonon phase velocities of acoustic branches, including TA1, TA2 and LA for (a) T6-carbon, (b) T10, (c) 3D-C5 along [100] and [001], as well as that for (d) diamond and (e) graphene.

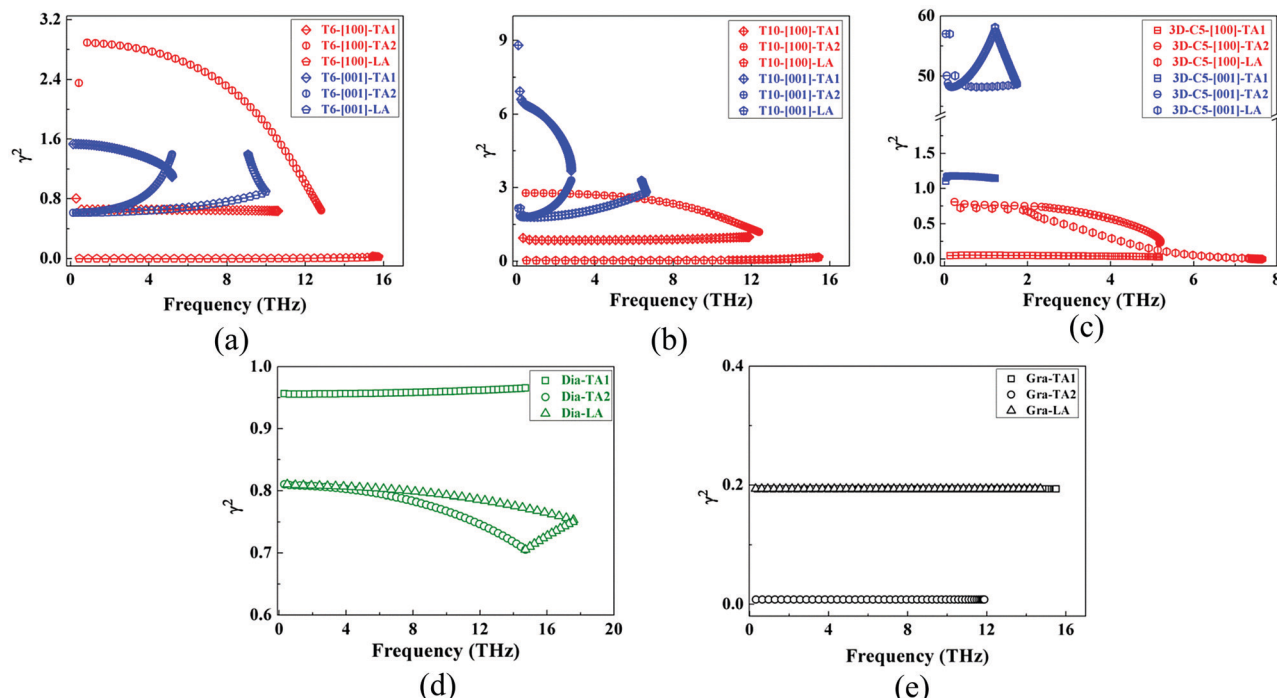


Fig. 6 Square of Grüneisen parameters γ^2 of acoustic branches, including TA1, TA2 and LA for (a) T6-carbon, (b) T10, (c) 3D-C5 along [100] and [001], as well as that for (d) diamond and (e) graphene.

angle, the two most fundamental properties of chemical bonds, on the thermal conductivity of carbon allotropes are concerned.

In a series of carbon allotropes, graphene and diamond have been the two materials with the highest thermal conductivity in

two-dimensional and three-dimensional materials till now, respectively, due to their ideal sp^2 (the bond length is 1.42 Å, and the bond angle is 120°) and sp^3 (the bond length is 1.54 Å and the bond angle is 109.47°) bonding structures. For the carbon allotropes studied in our work, their bonding structures have changed greatly when compared with graphene and diamond. Table 3 lists all the bond structures of T6-carbon, T10 and 3D-C5, as well as graphene and diamond, including their bond length properties (all the bond lengths, their corresponding bond types, and corresponding ratios) and bond angle properties (all the bond angles, their corresponding bond types, and corresponding ratios).

To obtain the relationship between bond structures and thermal conductivity in carbon allotropes, by taking the bond structures of graphene and diamond as standards, a new parameter δ , which we call the bond difference parameter (BDP), is defined in our work, and it is expressed as below:

$$\delta = \sum_{i=1}^n \{[(l_i - l_{sd})/l_{sd} \times r_l] + [(\alpha_i - \alpha_{sd})/\alpha_{sd} \times r_\alpha]\} \quad (7)$$

where l_i and α_i are all the different bond lengths and bond angles of carbon allotropes, respectively. l_{sd} and α_{sd} are the corresponding standard bond lengths and standard bond angles; for sp^2 bonds, l_{sd} is 1.42 Å and α_{sd} is 120°, and for sp^3 bonds, l_{sd} is 1.54 Å and α_{sd} is 109.47°. r_l and r_α are the ratios of different kinds of bond lengths and bond angles, respectively. It is apparent that the value of δ shows a degree of bond difference of carbon allotropes when compared with those of diamond and graphene. The larger δ is, the higher the bond difference is, and we predict that the thermal conductivity of carbon allotropes is low. To verify our prediction and obtain the BDP for T6-carbon, T10 and 3D-C5, all the parameters in Table 3 have been applied, and the calculated results are listed in the inset of Fig. 7. It can be seen that the BDP δ for T6-carbon

Table 3 Bond properties for T6-carbon, T10, 3D-C5, diamond and graphene, including their bond length properties (all the bond length, their corresponding bond type, and corresponding ratio) and bond angle properties (all the bond angle, their corresponding bond type, and corresponding ratio)

Name	Bond length (Å)	sp^2/sp^3	Ratio	Bond angle (°)	sp^2/sp^3	Ratio
T6-carbon	1.3419	sp^2	0.25	122.532	sp^2	0.25
	1.5435	sp^3	0.75	144.937	sp^3	0.25
T10				106.81	sp^3	0.5
	1.342	sp^2	0.14	122.629	sp^2	0.1
	1.518	sp^3	0.44	114.742	sp^3	0.2
3D-C5	1.57	sp^3	0.42	108.226	sp^3	0.4
				109.092	sp^3	0.1
				109.661	sp^3	0.2
Graphene	1.37	sp^2	0.28	140.06	sp^2	0.161
	1.446	sp^2	0.26	110.288	sp^2	0.355
	1.526	sp^3	0.46	109.652	sp^2	0.194
				114.339	sp^3	0.194
				100.121	sp^3	0.096
Diamond	1.42	sp^2	1	120	sp^2	1
Diamond	1.54	sp^3	1	109.47	sp^3	1

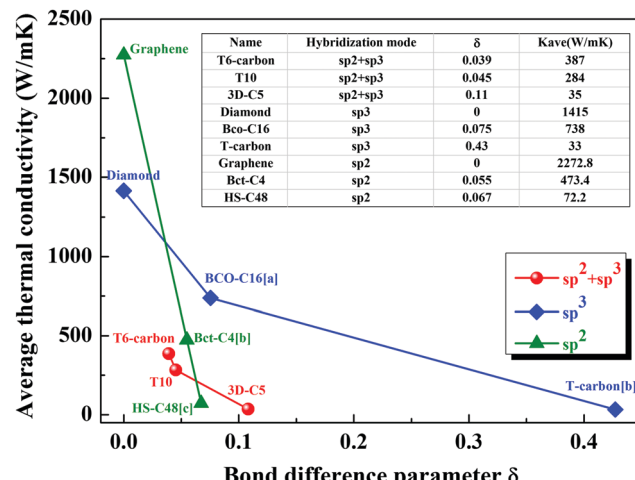


Fig. 7 Relationship between the average thermal conductivity and bond difference parameters for carbon allotropes with sp^2 and sp^3 hybridization (including T6-carbon, T10 and 3D-C5), carbon allotropes with all sp^2 hybridization (including graphene, Bct-C4 and HS-C48) and carbon allotropes with all sp^3 hybridization (including diamond, Bco-C16 and T-carbon). Inset table: the calculated bond difference parameters and the corresponding average thermal conductivity for carbon allotropes. [a] Ref. 33, [b] ref. 40, and [c] ref. 41.

is 0.045, and its corresponding average thermal conductivity K_{ave} is $284 \text{ W m}^{-1} \text{ K}^{-1}$, for T10, δ is 0.039, and K_{ave} is $387 \text{ W m}^{-1} \text{ K}^{-1}$, while for 3D-C5, δ is 0.11, and K_{ave} is only $35 \text{ W m}^{-1} \text{ K}^{-1}$. Although all of them have sp^2 and sp^3 hybridization, the values of BDP are rather different from each other, thus, leading to rather different thermal conductivities. It can also be observed in Fig. 7 that with the increase of BDP, the average thermal conductivity K_{ave} is decreased. We can infer that BDP is a factor to determine the thermal conductivity. The larger BDP, indicating that the closer the bond structures to diamond or graphene, meaning stiffer bonds,³³ corresponds to a higher ability of thermal transport of phonons or larger thermal conductivity of the formed carbon allotropes. Moreover, to further verify the universality of our relation, some other carbon allotropes, such as Bct-C4,³³ T-carbon,⁴⁰ Bco-C16⁴⁰ and HS-C48⁴¹ with different hybridizations, have also been applied, and thus, the relationship between δ and K_{ave} for carbon allotropes with all sp^2 hybridization (graphene, Bct-C4 and HS-C48) and all sp^3 hybridization (diamond, Bco-C16 and T-carbon) can also be observed in Fig. 7, and similar change rules between δ and K_{ave} can be found, validating our prediction further. Therefore, for carbon allotropes with the same hybridization, their thermal conductivities can be compared only by calculating their bond difference parameters δ , the larger the value of δ is, the lower the average thermal conductivity K_{ave} will be.

4. Conclusions

In summary, by combining NEMD simulations and phonon kinetic theory, thermal transmission in three novel carbon allotropes with sp^2 and sp^3 hybridization, including T6-carbon,

T10 and 3D-C5 at room temperature is studied. For comparison, graphene and diamond with standard sp^2 and sp^3 hybridization, respectively, are also studied. Our results indicate that the average thermal conductivities of T6-carbon, T10 and 3D-C5 at 300 K are much lower than those of diamond and graphene. Phonon kinetic theory analysis shows that the lower thermal conductivity of T6-carbon, T10 and 3D-C5 is caused by the combined action of their reduced phonon group velocities and relaxation time. Moreover, the different thermal conductivities of carbon allotropes can be described by the bond difference parameter. For carbon allotropes with the same hybridization, the larger the bond difference parameter is, the lower the average thermal conductivity will be. This parameter presents a new and convenient method for an in-depth understanding of the thermal transport properties of carbon allotropes.

Conflicts of interest

There are no conflicts to declare.

Acknowledgements

This work was supported by the National Natural Science Foundation of China (Grant No. 51771165), the Natural Science Foundation of Hebei Provincial Department of Education (Grant No. BJ2018052), the Open Foundation of State Key Laboratory of Metastable Materials Science and Technology (Grant No. 201804/201812), and the Japan Society for the Promotion of Science (JSPS) (Grant No. 19K14902).

References

- B. Ni, T. Watanabe and S. R. Phillpot, Thermal transport in polyethylene and at polyethylene–diamond interfaces investigated using molecular dynamics simulation, *J. Phys.: Condens. Matter*, 2009, **21**(8), 084219.
- H. S. Yang, G. R. Bai, L. J. Thompson and J. A. Eastman, Interfacial thermal resistance in nanocrystalline yttria-stabilized zirconia, *Acta Mater.*, 2002, **50**(9), 2309–2317.
- P. C. Millett, D. Wolf, T. Desai, S. Rokkam and A. El-Azab, Phase-field simulation of thermal conductivity in porous polycrystalline microstructures, *J. Appl. Phys.*, 2008, **104**, 033512.
- S. Iijima, Helical microtubules of graphitic carbon, *Nature*, 1991, **354**(6348), 56.
- J. Robertson, Diamond-like amorphous carbon, *Mater. Sci. Eng., R*, 2002, **37**(4-6), 129–281.
- X. L. Sheng, Q. B. Yan, F. Y. Ye, Q. R. Zheng and G. Su, T-carbon: a novel carbon allotrope, *Phys. Rev. Lett.*, 2011, **106**(15), 155703.
- X. J. Wei and Y. Yoshi, Stacked microchannel heat sinks for liquid cooling of microelectronic components, *J. Electron. Packag.*, 2004, **126**(1), 60–66.
- F. Q. Wang, J. Yu, Q. Wang, Y. Kawazoe and P. Jena, Lattice thermal conductivity of penta-graphene, *Carbon*, 2016, **105**, 424–429.
- L. D. Zhao, G. J. Tan, S. Q. Hao, Y. L. Pei, H. Chi and H. Wang, *et al.*, Ultrahigh power factor and thermoelectric performance in hole-doped single-crystal SnSe, *Science*, 2016, **351**(6269), 141–144.
- A. A. Balandin, Thermal properties of graphene and nanostructured carbon materials, *Nat. Mater.*, 2011, **10**(8), 569.
- H. C. Dong, B. Wen and R. Melnik, Relative importance of grain boundaries and size effects in thermal conductivity of nanocrystalline materials, *Sci. Rep.*, 2014, **4**, 7037.
- H. C. Dong, J. W. Xiao, R. Melnik and B. Wen, Weak phonon scattering effect of twin boundaries on thermal transmission, *Sci. Rep.*, 2016, **6**, 19575.
- A. Bagri, S. P. Kim, R. S. Ruoff and V. B. Shenoy, Thermal transport across twin grain boundaries in polycrystalline graphene from nonequilibrium molecular dynamics simulations, *Nano Lett.*, 2011, **11**(9), 3917–3921.
- A. A. Balandin, S. Ghosh, W. Bao, W. Z. Bao, I. Calizo and D. Teweldebrhan, *et al.*, Superior thermal conductivity of single-layer graphene, *Nano Lett.*, 2008, **8**(3), 902–907.
- S. Ghosh, I. Calizo, D. Teweldebrhan, E. P. Pokatilov, D. L. Nika and A. A. Balandin, *et al.*, Extremely high thermal conductivity of graphene: Prospects for thermal management applications in nanoelectronic circuits, *Appl. Phys. Lett.*, 2008, **92**(15), 151911.
- S. H. Zhang, Q. Wang, X. S. Chen and P. Jena, Stable three-dimensional metallic carbon with interlocking hexagons, *Proc. Natl. Acad. Sci. U. S. A.*, 2013, **110**(47), 18809–18813.
- Y. Q. Liu, X. Jiang, J. Fu and J. J. Zhao, New metallic carbon: Three dimensionally carbon allotropes comprising ultra-thin diamond nanostripes, *Carbon*, 2018, **126**, 601–610.
- C. Y. Zhong, Y. P. Chen, Z. M. Yu, Y. Xie, H. Wang and S. Y. Yang, *et al.*, Three-dimensional Pentagon Carbon with a genesis of emergent fermions, *Nat. Commun.*, 2017, **8**, 15641.
- F. Müller-Plathe and D. Reith, Cause and effect reversed in non-equilibrium molecular dynamics: an easy route to transport coefficients, *Comput. Theor. Polym. Sci.*, 1999, **9**(3–4), 203–209.
- F. Müller-Plathe, A simple nonequilibrium molecular dynamics method for calculating the thermal conductivity, *J. Chem. Phys.*, 1997, **106**(14), 6082–6085.
- S. Plimpton, Fast parallel algorithms for short-range molecular dynamics, *J. Comput. Phys.*, 1995, **117**(1), 1–19.
- L. Lindsay and D. A. Broido, Optimized Tersoff and Brenner empirical potential parameters for lattice dynamics and phonon thermal transport in carbon nanotubes and graphene, *Phys. Rev. B: Condens. Matter Mater. Phys.*, 2010, **81**(20), 205441.
- T. H. Liu, S. C. Lee, C. W. Pao and C. C. Chang, Anomalous thermal transport along the grain boundaries of bicrystalline graphene nanoribbons from atomistic simulations, *Carbon*, 2014, **73**, 432–442.
- X. Xu, L. F. C. Pereira, Y. Wang, J. Wu, K. W. Zhang and X. M. Zhao, *et al.*, Length-dependent thermal conductivity in suspended single-layer graphene, *Nat. Commun.*, 2014, **5**, 3689.

- 25 S. Berber, Y. K. Kwon and D. Tománek, Unusually high thermal conductivity of carbon nanotubes, *Phys. Rev. Lett.*, 2000, **84**(20), 4613.
- 26 H. Zhong and J. R. Lukes, Interfacial thermal resistance between carbon nanotubes: molecular dynamics simulations and analytical thermal modeling, *Phys. Rev. B: Condens. Matter Mater. Phys.*, 2006, **74**(12), 125403.
- 27 E. S. Landry and A. J. H. McGaughey, Thermal boundary resistance predictions from molecular dynamics simulations and theoretical calculations, *Phys. Rev. B: Condens. Matter Mater. Phys.*, 2009, **80**(16), 165304.
- 28 J. C. Zhang, Y. C. Wang and X. W. Wang, Rough contact is not always bad for interfacial energy coupling, *Nanoscale*, 2013, **5**(23), 11598–11603.
- 29 Y. Hong, L. Li, X. C. Zeng and J. C. Zhang, Tuning thermal contact conductance at graphene–copper interface *via* surface nanoengineering, *Nanoscale*, 2015, **7**(14), 6286–6294.
- 30 P. L. Garrido, P. I. Hurtado and B. Nadrowski, Simple one-dimensional model of heat conduction which obeys Fourier's law, *Phys. Rev. Lett.*, 2001, **86**(24), 5486.
- 31 A. Togo and I. Tanaka, First principles phonon calculations in materials science, *Scr. Mater.*, 2015, **108**, 1–5.
- 32 G. Kresse, J. Furthmüller and J. Hafner, Ab initio force constant approach to phonon dispersion relations of diamond and graphite, *EPL*, 1995, **32**(9), 729.
- 33 S. Y. Yue, G. Z. Qin, X. L. Zhang, X. L. Sheng, G. Su and M. Hu, Thermal transport in novel carbon allotropes with sp^2 or sp^3 hybridization: An ab initio study, *Phys. Rev. B*, 2017, **95**(8), 085207.
- 34 P. K. Schelling, S. R. Phillpot and P. Keblinski, Comparison of atomic-level simulation methods for computing thermal conductivity, *Phys. Rev. B: Condens. Matter Mater. Phys.*, 2002, **65**(14), 144306.
- 35 Z. Wang, J. E. Alaniz, W. Jang, J. E. Garay and C. Dames, Thermal conductivity of nanocrystalline silicon: importance of grain size and frequency-dependent mean free paths, *Nano Lett.*, 2011, **11**(6), 2206–2213.
- 36 X. Feng, J. W. Xiao, R. Melnik, Y. Kawazoe and B. Wen, Mechanical and thermal properties of γ -Mg₂SiO₄ under high temperature and high pressure conditions such as in mantle: a first principles study, *J. Chem. Phys.*, 2015, **143**(10), 104503.
- 37 E. S. Toberer, A. Zevalkink and G. J. Snyder, Phonon engineering through crystal chemistry, *J. Mater. Chem.*, 2011, **21**(40), 15843–15852.
- 38 H. C. Dong, B. Wen, Y. W. Zhang and R. Melnik, Low thermal conductivity in Si/Ge hetero-twinned superlattices, *RSC Adv.*, 2017, **7**(48), 29959–29965.
- 39 H. Y. Jin, O. D. Restrepo, N. Antolin, S. R. Boona, W. G. Windl and R. C. Myers, *et al.*, Phonon-induced diamagnetic force and its effect on the lattice thermal conductivity, *Nat. Mater.*, 2015, **14**(6), 601.
- 40 Z. Q. Ye, B. Y. Cao and Z. Y. Guo, High and anisotropic thermal conductivity of body-centered tetragonal C4 calculated using molecular dynamics, *Carbon*, 2014, **66**, 567–575.
- 41 W. D. Fu, Y. Zhang, J. C. Shang, L. Zeng and Y. X. Cai, Lattice thermal conductivity and bandgap engineering of a three-dimensional sp^2 -hybridized Dirac carbon material: HS-C48, *Comput. Mater. Sci.*, 2018, **155**, 293–297.